Assessing Digital Surface Models by Verifying Shadows: A Sensor Network Approach

Cláudio Carneiro[1], Mina Karzand[2], François Golay[1], Yue M. Lu[2] & Martin Vetterli[2]

[1] Geographical Information Systems Laboratory (LASIG), Ecole Polytechnique Fédérale de Lausanne (EPFL), Switzerland
Claudio.Carneiro@epfl.ch, Francois.Golay@epfl.ch
[2] Audiovisual Communications Laboratory (LCAV), Ecole Polytechnique Fédérale de Lausanne (EPFL), Switzerland
Mina.Karzand@epfl.ch, Yue.Lu@epfl.ch, Martin.Vetterli@epfl.ch

Abstract

We propose to use wireless sensor networks to assess the accuracy and application of Digital Surface Models (DSM) for the study of shadowing and solar radiation over the built environment. Using the ability of sensor network data to provide information about solar radiation and predicting the exact time of the day that the Sun starts radiating a sensor, a comparative study and statistical analysis can be undertaken in order to evaluate the accuracy of the DSM for shadowing and radiation studies using image processing techniques. Two DSMs of the EPFL campus with different cell resolutions (1 meter and 0.5 meters), considering only information about ground, buildings with vertical walls and trees, are constructed step by step and employed. Three DSMs of the same campus with a cell resolution of 1 meter derived from raw LIDAR data and common interpolation techniques, such as Triangulated Irregular Network (TIN), kriging, Inverse Distance Weighting (IDW), are also used for comparison.

Keywords: LIDAR point clouds, digital surface models, sensor network, shadowing

1 Introduction

Today's availability of 3-D information concerning cities enables the study of the urban framework in a new and more sophisticated approach. In fact, even though Airborne Light Detection and Ranging (LIDAR) data permits to derive valuable and accurate information about the physical arrangement of cities, not too many applications have been implemented in order to process this data for environmental analysis, such as shadowing and solar radiation, and hence, understanding the performance of the urban form. For instance, the growing importance given to the quantification of energy-based indicators at the scale of the city, strongly suggests the incorporation of 3-D geography in order to provide useful applications for the urban planning (Osaragi and Otani, 2007).

The analysis of shadowing and solar radiation in architecture and urban planning is a well-studied problem (Morello and Ratti, 2009). In fact, tools that can accurately calculate the radiation performance of buildings already exist, such as

RADIANCE lighting simulation model (Ward, 1994). Nevertheless, these tools are very useful at the micro-scale of architecture (environmental performance software) or at the macro-scale of landscape and regional geography (GIS tools), but the focus on urban district and tool for automatically calculating irradiation on a whole district are mostly lacking.

Airborne Laser Scanning (ALS), also called LIDAR, is a modern, fast and accurate technology that integrates sensors in order to obtain very accurate 3-D coordinates (x, y, z) data points located on the surface of the earth, such as ground points, buildings and trees. In order to establish the position of the sensor each time a point is measured, the Global Positioning System (GPS) is used. For finding out the attitude of the sensor, an Inertial Navigation System (INS) is adopted by using a narrow laser beam to determine the range between the sensor and the target points. Thus, using the capability of raw point clouds data derived from LIDAR technology and vectorial buildings footprints stored in a GIS, an accurate 2.5-D urban surface model, also called Digital Surface Model (DSM), can be constructed and further applied to the calculation of shadowing and radiation on urban fabric at neighbour/district scales.

In this paper we intend to validate the accuracy of the five gridded DSM of the EPFL campus, Lausanne, Switzerland, generated by different interpolation methods and techniques. The shadowing (i.e. solar radiation discontinuities) predicted by these DSMs are compared to the real solar radiation measurements obtained by a wireless sensor network deployed on the same campus.

Finally, we compute the average error between the transition time derived from the solar radiation measurements and that from shadowiness analysis using a DSM, validating the usefulness of DSMs for this type of environmental studies.

2 Related work

Previous literature on interpolation of LIDAR point clouds is not rare. The advantages and disadvantages of numerous interpolation methods, such as triangle-based linear interpolation, nearest neighbor interpolation and kriging interpolation were presented by Zinger *et al.* (2002). Control techniques that analyze the precision, accuracy and reliability of digital terrain models (DTM) and DSM can be carried out for applications where high level of accuracy is demanded (Menezes *et al.*, 2005), (Karel *et al.*, 2006), (Gonçalves, 2006).

The effects of LIDAR data density on the accuracy of digital elevation models and examination to what extent a set of LIDAR data can be reduced yet still maintain adequate accuracy for DEM generation were studied by Liu and Zhang (2008).

The source and nature of errors in digital elevation models, and in the derivatives of such models were studied by Fisher and Tate (2006). The recent advances of airborne LIDAR systems and the use of LIDAR data for DEM generation, with special focus on LIDAR data filters, interpolation methods, DEM resolution, and LIDAR data reduction were recently studied by Liu (2008). As related research, a quality improvement of laser altimetry of digital elevation models using a ground control points in a 1D strip adjustment was proposed by Elberink *et al.* (2003).

A method to interpolate and construct a DSM (incorporating the geographical relief), based on LIDAR and GIS buildings data, has already been proposed by Osaragi and Otani (2007). Also, two different studies concerning the analysis of solar potential of roofs using DSM have been recently presented (Kassner *et al.*, 2008; Beseničara *et al.*, 2008). As related research, there are some semi-automatic

methods available to create 3-D GIS data from LIDAR data, such as the Virtual London at UCL (Steed et al., 1999) and the MapCube at Tokyo CadCenter Corporation (Takase et al., 2003).

Furthermore, a group of researchers at the Martin Centre, University of Cambridge can be considered pioneers in the use of DSM to extract environmental indicators, as far as literature about the application of raster images in urban studies is concerned (Ratti, 2001; Ratti and Richens, 2004; Ratti *et al.*, 2005).

Today's growing accessibility of 3-D information from user generated contents and remote sensing surveys, makes this technique extremely useful for a common understanding of the performance of our cities. However, there is a lack of information concerning the accuracy of these models for this type of environmental analysis. Thus, in this work we aim to assess the accuracy of shadowing predictions made using these DSM through the comparison with real solar radiation measurements directly derived from sensor network data.

3 Construction and gridding interpolation of Digital Surface Models (DSM)

3.1 Presentation

The goal of gridding interpolation techniques is to generate, through spatial interpolation, on a regular basis, rectangular array of Z values derived from irregularly spaced XYZ data points. Many spatial interpolation methods are available and can be classified, such as:

- **Global**: each interpolated value, defined as a cell node of the gridded DSM, is influenced by all the data points, in this case raw LIDAR data in the form of XYZ point clouds.
- **Local**: each interpolated value is just influenced by the values at pre-defined nearby points of the XYZ point clouds.
- **Exact**: creates a surface that passes through all of the XYZ point clouds.
- **Approximate**: produces a surface that follow only a overall tendency in the XYZ point clouds in which there exists a few degree of error.
- **Stochastic**: incorporates geo-statistic theory in order to produce surfaces with particular levels of error.

In our testing areas at the EPFL campus, LIDAR points were obtained with a density of one point per square metre and only one LIDAR pulse. As presented by Behan (2000), the most accurate surfaces are achieved using a grid with a sampling size that matches as much as possible the LIDAR point density during the acquisition phase. Hence, four of the five gridding interpolation techniques here presented have a sampling size of 1 meter.

3.2 Gridding interpolation techniques

For large sets of LIDAR point clouds the grid computation of some global interpolation methods is too slow. However, these interpolation methods can be transformed into local by limiting the interpolation area to a neighbor area. Thus, in order to implement this project we gridded the following DSM with a sampling size of one meter:

- Three DSMs, derived from common local interpolation methods: inverse distance weighting (global interpolation), kriging (stochastic interpolation) and triangulation with linear interpolation (exact interpolation).
- One DSM, called 2.5-D Urban Surface Model (2.5-DUSM): interpolation technique is applied in different steps, such as presented in section 3.2.

A fifth DSM (second 2.5-DUSM), with a sampling size of 0.5 meters, was also used for comparison with all the other four DSMs having a sampling size of one meter.

Finally, all interpolated DSMs are slightly smoothed applying a 3 by 3 low-pass filtering.

3.2.1 Inverse Distance Weighting

Quite often the inverse distance weighting technique is used for interpolation of irregularly spaced points. In this method, the LIDAR point clouds are weighted during interpolation in order to decrease the influence of one point relative to another with distance from the grid node under analysis (Shepard, 1968). The main concept inherent to this technique is that nearby points have similar heights values, while the heights at faraway points are classified as being independent. Moreover, a weighting power that controls how the weighting factor drop off as distance from a grid node increases is usually assigned to data.

The generation of "bull's-eyes" surrounding the position of observations within the gridded area occurs after applying inverse distance weighting interpolation. Thus, a smoothing parameter can be applied during the interpolation process in order to reduce the "bull's-eye" output by smoothing the interpolated grid.

3.2.2. Kriging

Kriging is a geo-statistical interpolation technique that allows us to estimate the heights at the grid nodes as a weighted average of the measured heights at the reference points (LIDAR point clouds), usually in two steps: weight determination and the estimation of the height values using a weighted average. A procedure called variogram modeling which describes the spatial variability between the heights values of the reference points is used for the determination of weights (Cressie, 1993).

3.2.3 Triangulation with linear interpolation

The applied algorithm creates a triangulated irregular network (TIN) structure from the LIDAR points using a Delaunay Triangulation routine, which maximizes the minimum angle of all the angles of the triangles in the triangulation undertaken. The original points are connected in such a way that no triangle edges are intersected by other triangles. A sequential search allows the set up of a triangle in which each grid node is enclosed. The gradients of the picked triangle enables the interpolation of a value for the grid node (Franklin, 1973).

3.2.4 Construction and interpolation of a 2.5-D Urban Surface Model

Two data sources are required for the interpolation of the 2.5-D Urban Surface Model (2.5-DUSM) of the EPFL campus: raw LIDAR data and 2-D vectorial digital maps of buildings footprints stored in a GIS.
First, we interpolate a digital terrain model (DTM) by classifying the LIDAR points according to the following sequential operations:

- Using GIS software, LIDAR points confined within building polygons and in the 1 meter buffer generated from building polygons are eliminated.
- In a neighbourhood of 2 meters LIDAR points whose elevation value varies significantly from surrounding points are considered to be points indicating features such as aerial points (e.g., if the laser beam touches a bird) and vehicles, and thus are removed.

After eliminating the points based on the features described above, a DTM can be interpolated only from ground points. Due to its generalized use by the scientific community for DTM interpolation, the triangular interpolation (construction of a TIN) was chosen.

Secondly, we proceed as follows:

- Using only the LIDAR points classified as being contained within vectorial buildings footprints, a triangular interpolation (construction of a TIN) is independently applied to each of these buildings roofs. It is important to note that along the edges of the roofs, there exist some laser points touching walls and not roofs, which may influence the TIN generation of each roof. Thus, wall points need to be detected. A building point is classified as wall point if there are much higher points and none or very few points that have its approximate height in a neighborhood of 2 meters. Finally, construction of 2.5-D surface model of buildings with vertical walls is applied.
- LIDAR points considered to be trees higher than five meters are classified and further on construction of the 2.5-D surface model of trees. The algorithm used for this classification was initially presented by Axelsson (1999).

For each grid cell considered to be building or tree, its height (also defined as nDSM of buildings and trees) is taken to be the value of the difference between the terrain elevation (calculated in the interpolated DTM) and the buildings and trees elevation.

Lastly, each building and tree is added to the DTM, using the height found previously for each cell contained within, as described in last paragraph. The final result allows the construction of a 2.5-DUSM: DTM + nDSM of buildings with vertical walls + nDSM of trees. Data source and parameters needed to generate the 2.5-DUSM are shown in figure 1.

Finally, in order to complete the image enhancement of the model, we have to refine the facades of buildings that are slightly sloped because of interpolation. Thus, each building's contour pixel was deleted and then expanded again, in order to assign more constant values to roofs edges.

An example of a 2.5-DUSM of the EPFL campus, at the city of Lausanne, Switzerland, is shown on the right picture of Figure 2.

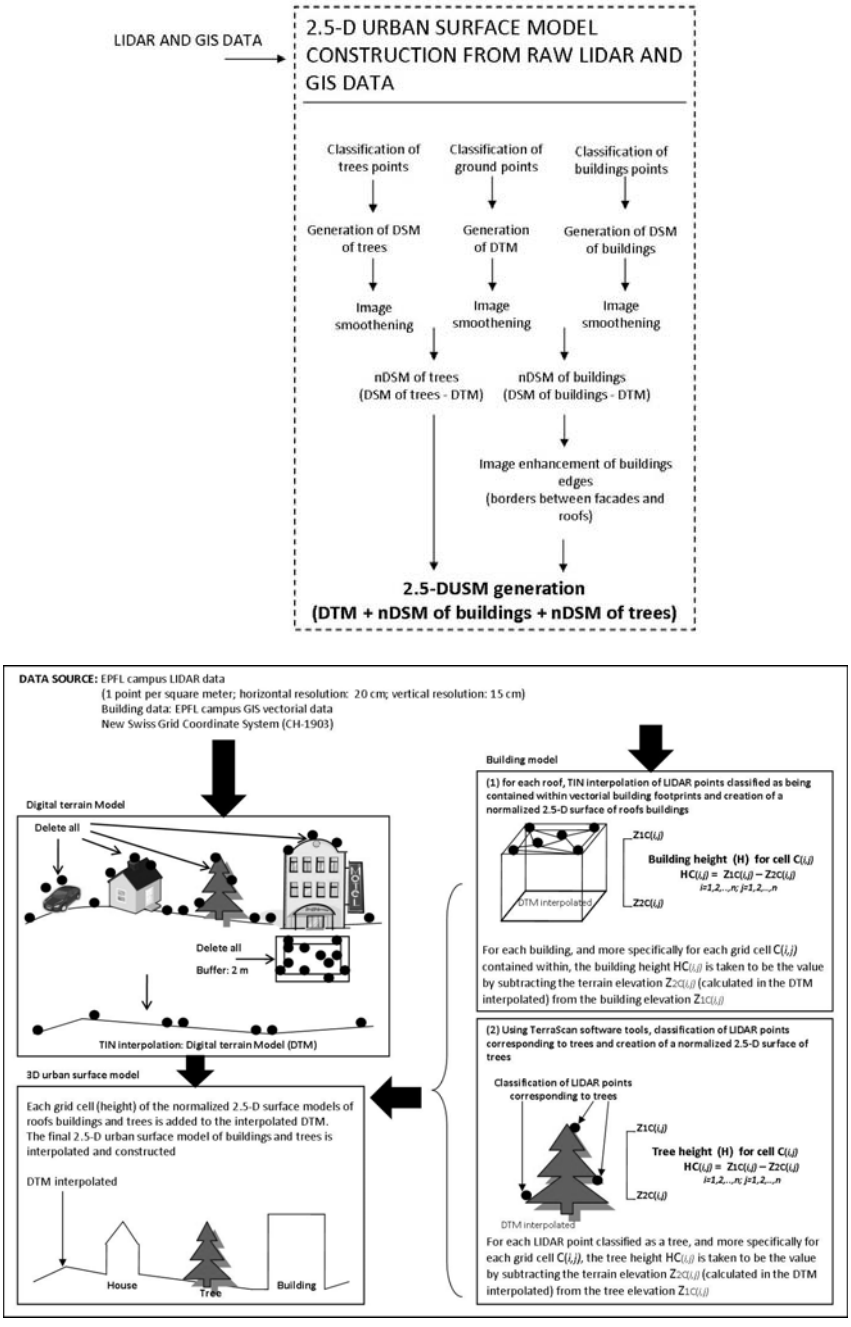

Figure 1. Blackbox (image above) and technique applied (image below) for the construction of a 2.5-D urban surface model (2.5-DUSM) with information of ground, buildings with vertical walls and trees.

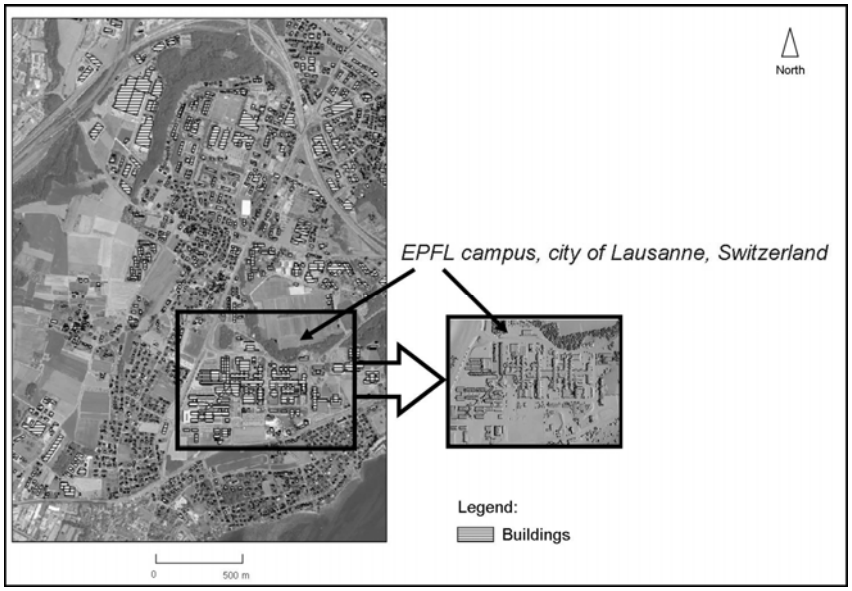

Figure 2. Left picture: GIS building footprints and aerial pictures of the district of Chavannes and EPFL campus, city of Lausanne, Switzerland; right picture: 2.5-D urban surface model (2.5-DUSM) of the EPFL campus, city of Lausanne, Switzerland; black rectangle: case study (pilot zone), within the EPFL campus, city of Lausanne, Switzerland.

4. SensorScope project

As presented by Barrenetxea *et al.* (2008), SensorScope is a joint project between network, signal processing, and environmental researchers that aims to provide a cheap and out-of-the-box environmental monitoring system based on a wireless sensors network. It has been successfully used in a number of deployments to gather hundreds of megabytes of environmental data. The geographical position of all the wireless sensors network of the EPFL campus was originally defined in WGS84 coordinates (GPS measurements) and later transformed into New Swiss Grid (CH-1903 datum) coordinates. The location and labeling (identification) of each sensor of the EPFL campus wireless sensor network is shown in Figure 3.

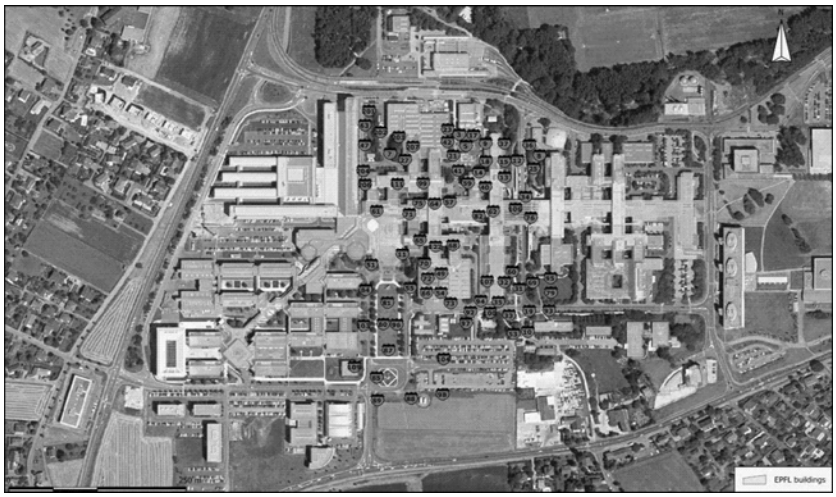

Figure 3. Position and identification of the wireless sensors network at the EPFL campus, city of Lausanne, Switzerland.

5. Presentation of the accuracy validation methodology

In order to validate the accuracy of the DSM presented before, the predictions based on map are compared with real measurements of solar radiation measured by sensors. The solar radiation parameter depends greatly on the amount of existing clouds during the day. In cloudy or rainy days the density of clouds in front of the sun determines how much solar radiation is received by the sensor. Thus, as a result of the disordered nature of the water drops in clouds, the measured solar radiation is a very chaotic signal. Contrarily, in sunny days, measured solar radiation is a piece-wise smooth signal which increases from morning to noon and decreases from noon to evening. The only irregularity in this signal is some jumps and drops in the level of the measured solar radiation. By jumps and drops, we mean there is a sudden increase or decrease in the level of signal over a very short time interval. The reason of existence of these jumps and drops is shadowing phenomena, i.e., whenever a sensor gets out of shadow, the solar radiation measured by it increases a lot in a short amount of time and whenever it goes into the shadow, the measured solar radiation drops suddenly. The main idea of the project was to use the DSM to predict the exact times of changing of shadowing for each sensor position (XYZ coordinates) on each sunny day and compare this prediction to the jumps and drops of the sensor measurements, such as presented in Figure 4.

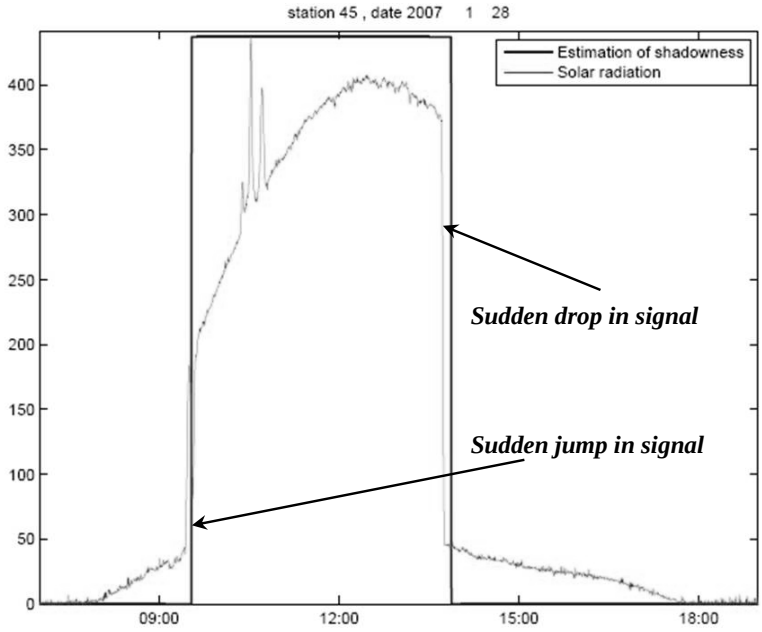

Figure 4. Comparison, on a sunny day, between the estimated shadowiness for a sensor position (XYZ coordinates) using a DSM and the solar radiation information of the same sensor.

As shown in Figure 4 there is no perfect match between the two independent parameters: estimation of shadowiness for a sensor position (XYZ coordinates) using DSM and solar radiation measured by sensors. Due to the fact that the prediction of shadowiness uses the DSM as its input data and as we may be somewhat confident about the times of jumps and drops read from sensor measurements, the error will most likely be caused by the existing errors on DSM. Thus, this error might be considered as a good measure of the quality of the DSM. A back tracing algorithm was used to estimate the shadow-state of each sensor at each time instant. Based on the day of the year and the latitude and longitude of the city of Lausanne, the algorithm calculates the exact direction of the Sun for each sensor at each moment and back-traces the ray of light from the sensor toward the Sun. Then, the height of this ray of light is compared to the curve derived from the DSM, which shows the elevation along the line in the same direction, as shown in Figure 5.

If there is any intersection where the ray of light is below the elevation according to the DSM, the point of that intersection will cast shadow on the corresponding sensor at that moment.

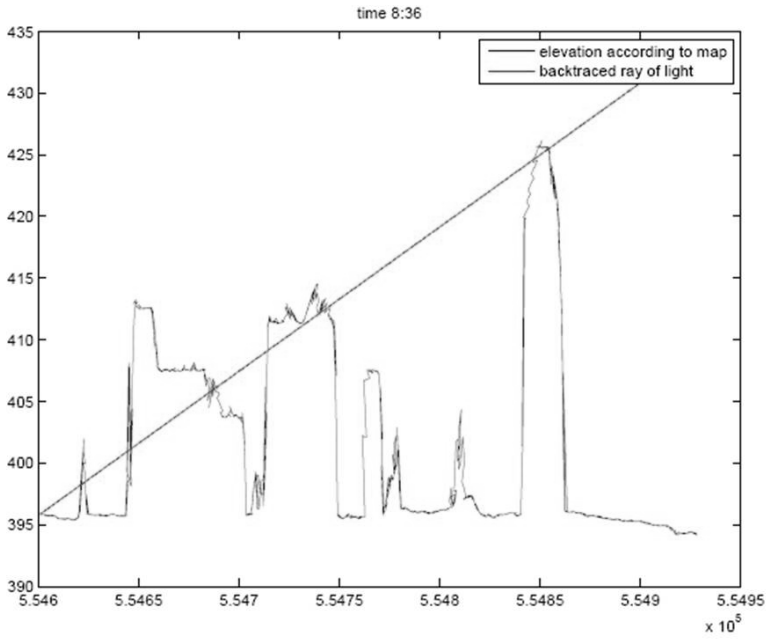

Figure 5. Comparison between the height of the ray of light, which is back-traced towards the Sun, and the elevation values of the DSM.

An illustrative representation of a theoretical shadow-map of EPFL campus at some time instant is presented in Figure 6. The direction of light coming from the sun is also shown in this figure.

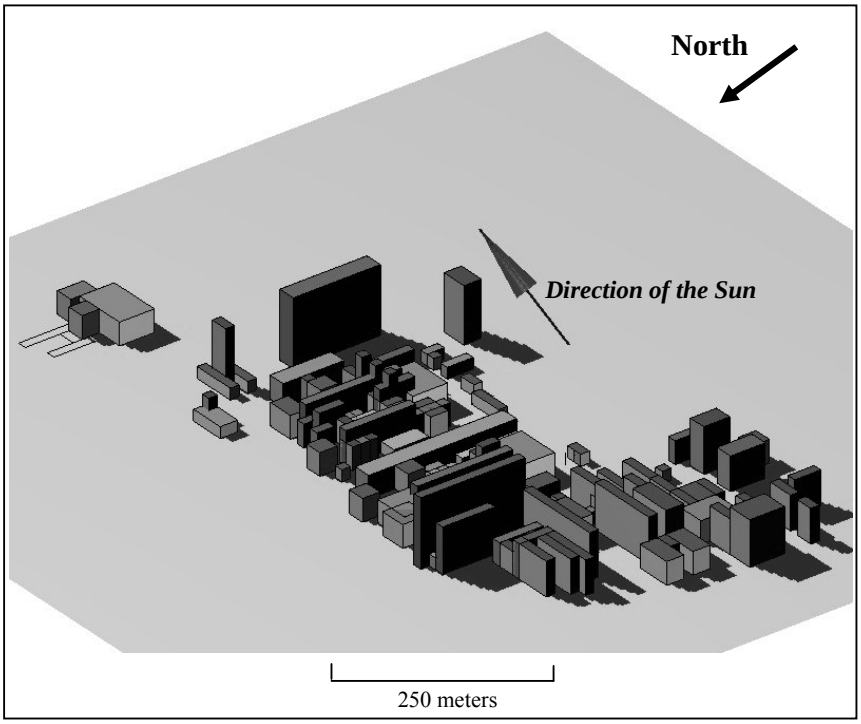

Figure 6. For some time instant and the direction of Sun, illustrative presentation of the theoretical shadow-map in the EPFL campus.

6. Analysis of results

The prediction of shadowiness is undertaken according to different DSMs and the measurements of solar radiation for each sensor in eight sunny days distributed along the year. Two parameters are introduced as a measure of accuracy (deviation and number of jumps and drops) between the application of DSM for shadowiness analysis for a sensor position (XYZ coordinates) using image processing techniques and the solar radiation information of sensors:

- **Number of jumps and drops** that could be predicted approximately for a threshold of 30 minutes. This threshold was defined in order to exclude all cases of sensors presenting an unstable behavior concerning solar radiation measurements – for most of the cases these sensors are at short distances from trees, where the shadowiness factor caused by the natural movement of leaves of trees is not negligible. Moreover, the classification and interpolation of trees is a complex issue on DSM interpolation. In this case mainly because the density of 1 point per square meter of LIDAR points available is too low. For this reason, the estimation of shadowiness caused by trees using DSM image processing techniques is also highly influenced by the quality of the interpolated DSM. In Figure 7 an example of a sensor with a fuzzy performance that could not be used for this classification is shown.

- **Average deviation error (in minutes)** for those jumps that could be predicted for a threshold of 30 minutes. The error is defined as the difference of time between jumps in solar radiation and boundaries of shadowiness, which are predicted according to the DSM.

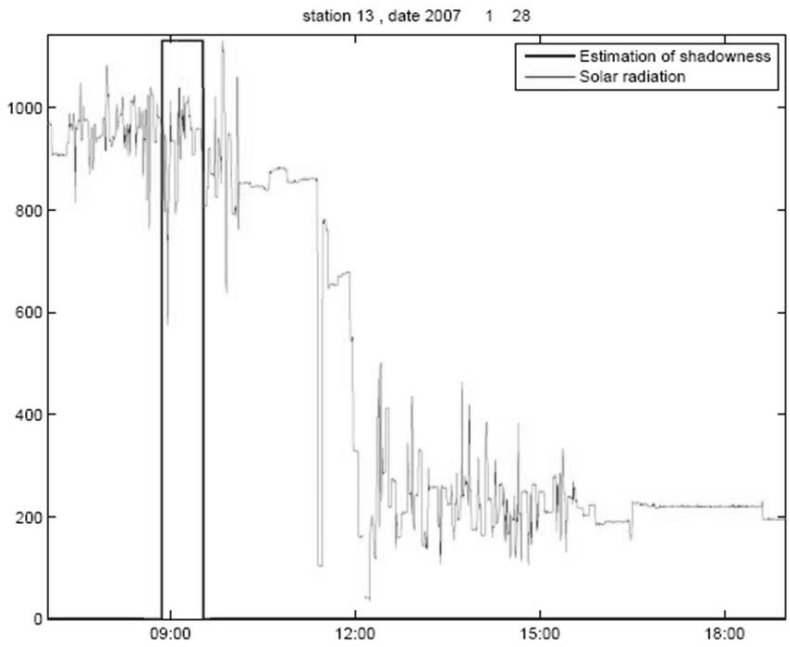

Figure 7. Example of a sensor with a fuzzy performance: solar radiation line.

- **Average spatial error on the vertical direction (in centimeters).** By using the timing errors of prediction of shadow and some geometrical assumptions on the environment, a spatial error parameter could also be defined. The imperfect matching of the prediction and sensor readings are because of error in interpolated value for elevation of dome points. By having the angle of sun in the predicted time and in the real time of the shadow transition and the vertical distance of the sensor and the obstruction point, the error in height of the obstruction point could be estimated. Corresponding to the Figure 8, assume that the position of the sensor is in point *O*. Based on the information in DSM, point *A* is assumed to cast shadow on the sensor at time t_1. So the angle of sun at this time is Φ. And the ray of light is assumed to be the line *AO*. But the measurements show that the shadow transition happens at time instant t_2 in which the sun has the angle of ψ for the point *O*. Thus the real ray of light that causes transition in shadow state of point *O* is *BO*. The error in estimating the shadow transition is because of the error in defining the elevation which is *AB*. Using simple geometry, we find the spatial error as:

$$\text{Spatial error} = |AB| = (\tan(\psi)-\tan(\Phi)) \times d$$

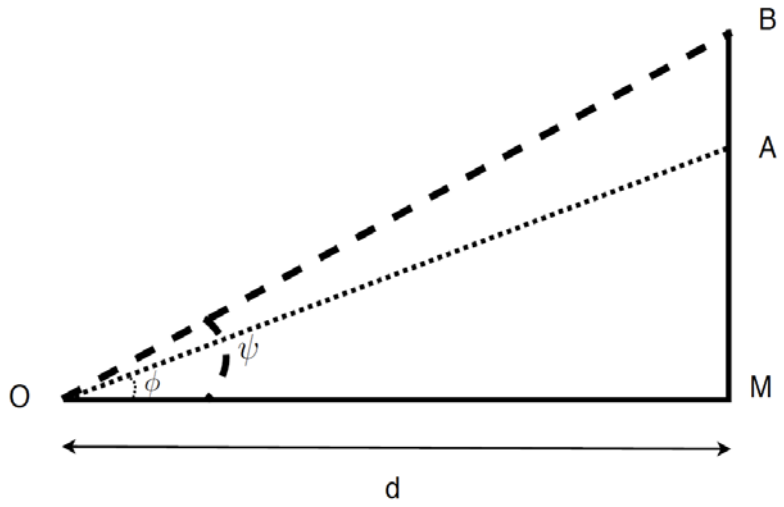

Figure 8. The model used for estimating the spatial error on the vertical direction of the DSM. The sensor is at point *O*. The model predicts the transition to happen at time t_1 when the sun has horizontal angle Φ, but the real transition happens at time t_2 corresponding to angle ψ.

Thus, for each transition in shadow state, a temporal error and a spatial vertical error could be defined. The simulation results of the average deviation error (in minutes), the number of jumps and drops and the average vertical spatial error (in centimeters) for each kind of the five DSM under analysis is presented in table1.

Table 1. Average Deviation Error (minutes), Number of Jumps and Drops and Average Vertical Spatial Error (centimeters) for each DSM under assessment.

DSM	**Average Deviation Error: (minutes)**	**Number of Jumps and Drops (threshold: 30 minutes)**	**Average Vertical Spatial Error: (cm)**
2.5-DUSM (1 meter of resolution)	4.57	85	26
2.5-DUSM (0.5 meters of resolution)	5.14	85	16
IDW (1 meter of resolution)	6.17	76	22
Kriging (1 meter of resolution)	5.19	77	19
TIN (1 meter of resolution)	6.19	85	19

From the analysis of Table 1 we can observe that the average deviation error of the 2.5-DUSM with 1 meter of resolution presents slightly better results than all the other DSM. In this case, according to the construction method applied and contrary to the other interpolations methods used (IDW, Kriging and TIN) the edges of roofs are more accurately defined. Hence, this will affect the propagation of shadowiness over the built environment using the DSM (2.5-DUSM) and will also implicitly improve its final accuracy. The 2.5-DUSM with a sampling size of 0.5 meters presents slightly worse results than the 2.5-DUSM with a sampling size of 1 meter. Once again, this can be caused by the fact that the density of LIDAR points used for this classification is equal to one point per square meter, and according to Behan (2000) the most accurate surfaces are created using a grid with a sampling size that relates as close as possible to the LIDAR point density during the acquisition phase, which means a grid with a sampling size of 1 meter.

Note that, as the mapping between the vertical spatial error and the temporal error can differ markedly from one sensor to the other, there exists no simple relationship between the average vertical error and the average temporal error reported in Table. 1. The average spatial error is strongly influenced by the distance parameter. Thus, the 2.5-DUSM with a higher resolution, here constructed with a sampling size of 0.5 meter, presents slightly better results than all the other DSMs under analysis, which have a coarser sampling size of 1 meter.

7. Conclusions

Using solar radiation measurements taken by a wireless sensor network, we present an algorithm for evaluating the quality and usefulness of five different DSMs in shadowiness and solar radiation studies on urban areas.

The results of this work show that there is no great difference among the four interpolation methods using a grid with a sampling size of 1 meter. The 2.5-DUSM presented here is the most robust method and for this reason its use should be generalized for this kind of environmental applications at neighbor/district cities scales.

We found that existing vectorial digital maps (GIS data) can be used if available and updated, but outlines of buildings from this source of information should always be handled with special care. In fact, the 2-D outlines of buildings footprints do not have to represent the outline of the building roof. Modifications between GIS data and laser data can have numerous reasons which cannot be automatically recognized. Proposals using vectorial digital maps as input for 2.5-D urban surface model interpolation and construction should be attentive of the fact that in some cases map information might not give the correct hints about 3-D buildings shapes.

Finally, some improvements concerning the technical implementation of the presented methodology are needed in future work, specially:

- The development of an algorithm for the automatic selection of solar radiation information for sensors presenting a smooth signal (sunny days).
- The use of modern LIDAR datasets with higher density of points per square meter and different signal pulses will allow to achieve better results. Thus, it will be possible to improve the classification and reconstruction of trees (using all pulses) and buildings (using first and last pulses) for the 2.5-DUSM here presented and also the reconstruction of DSM with denser and more accurate sampling size, such as 0.5 meters.

References

Axelsson, P. (1999), "Processing of laser scanner data - algorithms and applications". *ISPRS Journal of Photogrammetry and Remote Sensing*, Vol. 54, pp. 138– 147.

Barrenetxea, G., F. Ingelrest, Y. M. Lu and M. Vetterli. (2008), "Assessing the challenges of environmental signal processing through the SensorScope project", *Proceedings of the IEEE International Conference on Acoustics, Speech and Signal Processing*, Las Vegas, USA, pp. 5149-5152.

Behan, A. (2000), "On the matching accuracy of rasterised scanning laser altimetre data". *Proceedings of the ISPRS Congress 2000*, Vol. 33, Part B2, Amsterdam, pp. 75-82.

Beseničara, J., B. Trstenjak and D. Setnikac. (2008), "Application of Geomatics in Photovoltaics". *The International Archives of the Photogrammetry, Remote Sensing and Spatial Information Sciences*, Vol. 37, Part B4, pp.53-56.

Cressie, N. (1993), *Statistics for Spatial Data*. John Wiley & Sons, New York, USA.

Elberink, S., G. Brand and R. Brügelmann. (2003), "Quality improvement of laser altimetry DEM's". *Proceedings of the ISPRS working group III/3 workshop "3-D reconstruction from airborne laserscanner and InSAR data"*, October 8th-10th, Dresden, Germany (no pagination).

Fisher, P. and N.J. Tate. (2006), "Causes and consequences of error in digital elevation models". *Progress in Physical Geography*, Vol. 30, No. 4, pp. 467-489.

Franklin, W.R. (1973), "Triangulated irregular network program". ftp://ftp.cs.rpi.edu/pub/franklin/tin73.tar.gz

Gonçalves, G. (2006), "Analysis of interpolation errors in urban digital surface models created from LIDAR data". *Proceedings of the 7th International Symposium on Spatial Accuracy Assessment in Resources and Environment Sciences*. M. Caetano and M. Painho (eds.), Sana Hotel, July 5th-7th, Lisbon, Portugal, pp. 160-168.

Karel, W., N. Pfeifer and C. Briese. (2006), "DTM quality assessment". *The International Archives of Photogrammetry, Remote Sensing, and Spatial Information Sciences*, Vol. 36, Part 2, pp. 7-12.

Kassner, R., W. Koppe, T. Schüttenberg and G. Bareth. (2008), "Analysis of the Solar Potential of Roofs by Using Official LIDAR data". *The International Archives of the Photogrammetry, Remote Sensing and Spatial Information Sciences*, Vol. 37, Part B4, pp. 399-404.

Liu, X. (2008), "Airborne LIDAR for DEM generation: some critical issues". *Progress in Physical Geography*, Vol. 32 No. 1, pp. 31-49.

Liu, X. and Z. Zhang. (2008), "LIDAR data reduction for efficient and high quality DEM generation". *The International Archives of the Photogrammetry, Remote Sensing and Spatial Information Sciences*, Vol. 37, Part B3b, pp. 173-178.

Menezes, A.S., F.R. Chasco, B. Garcia, J. Cabrejas and M. González-Audícana, (2005), "Quality control in digital terrain models". *Journal of Surveying Engineering*, Vol. 131, pp. 118-124.

Morello, E. and C. Ratti. (2009), "SunScapes: 'solar envelopes' and the analysis of urban DEMs, Computers", *Environment and Urban Systems*, Vol. 33, Part 1, pp. 26-34.

Osaragi T. and I. Otani. (2007), "Effects of ground surface relief in 3D spatial analysis on residential environment". *The European Information Society: Lecture notes in Geoinformation and Cartography*, S. I. Fabrikant and M. Wachowicz (eds.), Springer, Berlin, Germany, pp. 171-186.

Ratti, C. (2001), *Urban analysis for environmental prediction*, unpublished Ph.D. dissertation, University of Cambridge, Cambridge, UK.

Ratti, C. and P. Richens. (2004), "Raster analysis of urban form". *Environment and Planning B: Planning and Design*, Vol. 31, Part 2, pp. 297-309.

Ratti, C., N. Baker and K. Steemers. (2005), "Energy consumption and urban texture". *Energy and Buildings*, Vol. 37, No. 7, pp. 762-776.

Shepard, D. (1968), "A two-dimensional interpolation function for irregularly-spaced data". *Proceedings of the 1968 ACM National Conference*, pp. 517–524.

Steed, A., E. Frecon, D. Pemberton and G. Smith. (1999), "The London Travel Demonstrator", *Proceedings of the ACM Symposium on Virtual Reality Software and Technology*, ACM Press, December 20th-22nd, pp. 50-57.

Takase, Y., N. Sho, A. Sone, , K. Shimiya. (2003), "Automatic generation of 3D city models and related applications". *The International Archives of the Photogrammetry, Remote Sensing and Spatial Information Sciences*, Vol. XXXIV-5/W10 (no pagination).

Ward, G. J. (1994), "The Radiance Lighting Simulation and Rendering System", *Journal of Computer Graphics: Proceedings of the Annual SIGGRAPH Conference*, pp. 459-472.

Zinger, S., M . Nikolova, M. Roux and H. Maître. (2002), "3-D resampling for airborne laser data of urban areas". *The International Archives of the Photogrammetry, Remote Sensing and Spatial Information Sciences* , Vol. 34, Part 3B, pp. 55-61.